Arabian Journal of Chemistry (2021) **14**, 103236

King Saud University

Arabian Journal of Chemistry

www.ksu.edu.sa
www.sciencedirect.com

ORIGINAL ARTICLE

Potential antidiabetic molecule involving a new chromium(III) complex of dipicolinic and metformin as a counter ion: Synthesis, structure, spectroscopy, and bioactivity in mice

Jin-long Dong [a,b,*], Bin Wen [a], Zhen Song [a], Jie Chai [c], Bin Liu [b], Wen-juan Tian [d], Gang Liang [e], Bin-sheng Yang [b,*]

[a] *Department of Chemistry, Taiyuan Normal University, Jinzhong 030619, China*
[b] *Institute of Molecular Science, Key Laboratory of Chemical Biology of Molecular Engineering of Education Ministry, Shanxi University, Taiyuan 030006, China*
[c] *College of Chemistry and Chemical Engineering, Jinzhong University, Jinzhong 030619, China*
[d] *Nanocluster Laboratory, Institute of Molecular Science, Shanxi University, Taiyuan 030006, China*
[e] *Department of Pathology, First Hospital of Shanxi Medical University, Taiyuan 030001, China*

Received 2 April 2021; accepted 25 May 2021
Available online 29 May 2021

KEYWORDS

Chromium(III) complex;
Metformin;
Diabetes mellitus;
Bioactivity

Abstract The chromium(III) complex, $Cr(C_7H_3NO_4)_2{\cdot}C_4H_{12}N_5$ (***1***), was synthesised by chelating chromium with dipicolinic (H_2dipic) in methanol, and its structure was characterised using elemental analysis (EA), spectroscopy (infrared, UV–visible, and fluorescence) and single-crystal X-ray method. The density functional theoretical (DFT) computation was performed using the Gaussian 09 package. The stability of solution at different temperatures and pH values, the electrochemical, morphological and thermal properties of complex ***1*** were discussed. The preliminary bioactivities of complex ***1*** in streptozotocin (STZ)-induced type 2 diabetes mellitus (T2DM) mice were investigated using daily oral gavage for 12 weeks. The cytotoxicity was assessed using the methyl thiazolyl tetrazolium (MTT) assays, and the acute toxicity experiment test was carried out on healthy C57BL/6 mice with this complex. The complex ***1*** crystallised in the monoclinic system with the space group P2(1)/n, R_1 = 0.0642. The DFT-optimised structure of complex ***1*** was in excellent agreement with

* Corresponding authors at: Institute of Molecular Science, Key Laboratory of Chemical Biology of Molecular Engineering of Education Ministry, Shanxi University, Taiyuan 030006, China.
E-mail addresses: dongjinlong20123@163.com (J.-l. Dong), yangbs@sxu.edu.cn (B.-s. Yang).
Peer review under responsibility of King Saud University.

Production and hosting by Elsevier

https://doi.org/10.1016/j.arabjc.2021.103236

the X-ray crystal structure. The complex ***1*** exhibited good physical and chemical properties and beneficial function on blood glucose and lipid metabolism for T2DM. The antidiabetic activity of chromium(III) might be associated with chromium(VI). Furthermore, the cytotoxicity and the acute toxicity experiments showed that the complex ***1*** was hypotonic and secure to organism. The study of complex ***1*** showed that the prepared complex on the basis of H_2dipic and Met could inhibit hyperglycaemia and hyperlipidaemia in *vivo* and did not have potential toxicity. These results demonstrated that the complex ***1*** might provide an important reference for the development of functional hypoglycaemic foods or pharmaceuticals of T2DM.

1. Introduction

The diabetes mellitus (DM) is the most important public disease after cancer and cardiovascular disease. Despite lifestyle modification and pharmacotherapy, the blood glucose control of patients with T2DM aggravates over time due to the continuous function deterioration of the pancreatic β-cell. In this respect, a durable glycaemic control is difficult to obtain for quite a long time with current drug treatment options Li et al., 2017; Forslund et al., 2015; Després and Lemieux, 2006; Robles et al., 2017. Therefore, the development of some functional supplements to prevent T2DM has become a research hotspot, such as functional compounds containing vanadium(VI), zinc(II) and chromium(III), among which the selection of ligands is particularly important Peng and Yang, 2015.

Clinically, metformin (Met), a cheap oral antihyperglycaemic biguanide agent, is widely used to treat T2DM over the last four decades. Met lowers blood glucose levels without the side effects of hyperinsulinaemia and gaining weightBen Sahra et al., 2010. Met metal complexes play an important role in biology, and its chemical structure in aqueous solution is dependent on pH. Four forms of Met are present in aqueous solution with different pH values, namely, diprotonated (H_2Met^{2+}) in strong acid, monoprotonated ($HMet^{+}$) in weak acid, neutral Met and deprotonated (Met^{-}) in strong alkaline solution (**Figure S1**). Therefore, Met coordinates as unidentate ligand via $N^{3\#}$ atom in a cationic form in general Lemoine et al., ; Zhu et al., (2002); more as a bidentate chelating ligand via $N^{2\#}$ and $N^{4\#}$ atom both in neutral as well as in anionic form Olar et al., (2006); Bentefrit et al., (1997); Olar et al., (2010); Al-Saif and Refat, (2013). In addition, Met can be found as a counter cation in individual complexes Lemoine et al., ; He et al.,.

The 2,6-pyridine dicarboxylic acid (dipicolinic acid or H_2-dipic) is an effective bidentate-or tridentate-chelating ligand that forms stable complexes with most metal ions (Aghabozorg et al., 2008). The dipicolinic acid exists in various natural compounds and shows potential pharmacological activity and different biological functions (Eshtiagh-Hosseini et al., 2010). At present, complexes involving H_2dipic and Met as counter ion or ligands and Zn(II) or Pd(II) as central metal ions have been reported (Ghasemi et al., 2014; Moghimi et al., 2011).

In the 1950 s, the trivalent chromium is first reported to play an important role in controlling blood glucose and proposed to be an essential trace element of biology Schwarz and Mertz, (1959). Then, low-molecular weight chromebinding peptide are considered as a biologically active form of Cr(III) in mammals. Subsequently, numerous studies on its potential role in maintaining homeostasis of blood glucose and lipid metabolism have been published Schwarz and Mertz, 1957. Laboratory and clinical studies also prove that pharmacologically related doses of Cr(III) can improve the insulin sensitivity and triglyceride and cholesterol levels in animals with obesity and T2DM, and increase insulin binding to cells Cefalu and Hu, (2004). Although the status of Cr(III) has recently been challenged Jain et al., 2006; Anderson, 2000; the Cr(III) has been an artificial second messenger in action of insulin Di Bona et al., (2011); Vincent, (2013). Given the low bioavailability of Cr(III) salts, new organic Cr(III) compounds should be designed, and their bioactivity should be explored. Thus, various forms of Cr(III) supplements, such as CrNic (Levina et al., 2016); CrPic (Vincent, 2015; Liu et al., 2015) and CrPro (Preuss et al., 2008; Kim et al., 2004**);** have been successfully applied in the market.

Based on the aforementioned considerations, we consider the synergistic effect on the Met and H_2dipic as suitable ligands for metal complexation to further improve its pharmacological and biological activities. Herein, $Cr(C_7H_3NO_4)_2{\cdot}C_4H_{12}N_5$, complex ***1*** is successfully prepared, thereby adding a new member to the family of organic Cr(III). The bioactivities and the toxicity of complex ***1*** are evaluated in T2DM mice. Surprisingly, the preliminary studies suggest that this complex may be a candidate for a promising new type of nontoxic antidiabetic drug. The concrete process is described in Fig. 1.

2. Materials and methods

2.1. Materials

All chemical reagents and solvents were of standard analytical grade and used without further purification unless otherwise stated, and all manipulations were performed under aerobic conditions. The dulbecco's modified eagle medium (DMEM) and the methyl thiazolyl tetrazolium (MTT) were purchased from Ruibo Biological technology co. LTD (Guangzhou, China). The Human breast cancer cells (MCF-7) were provided by the Gene Biology Center of Shanxi University. Human serum albumin (HSA) was purchased from Solarbio Life Sciences.

2.2. Methods

The crystal data for the compound were collected using the *SMARTAPEX* X-ray single-crystal diffractometer (Bruker

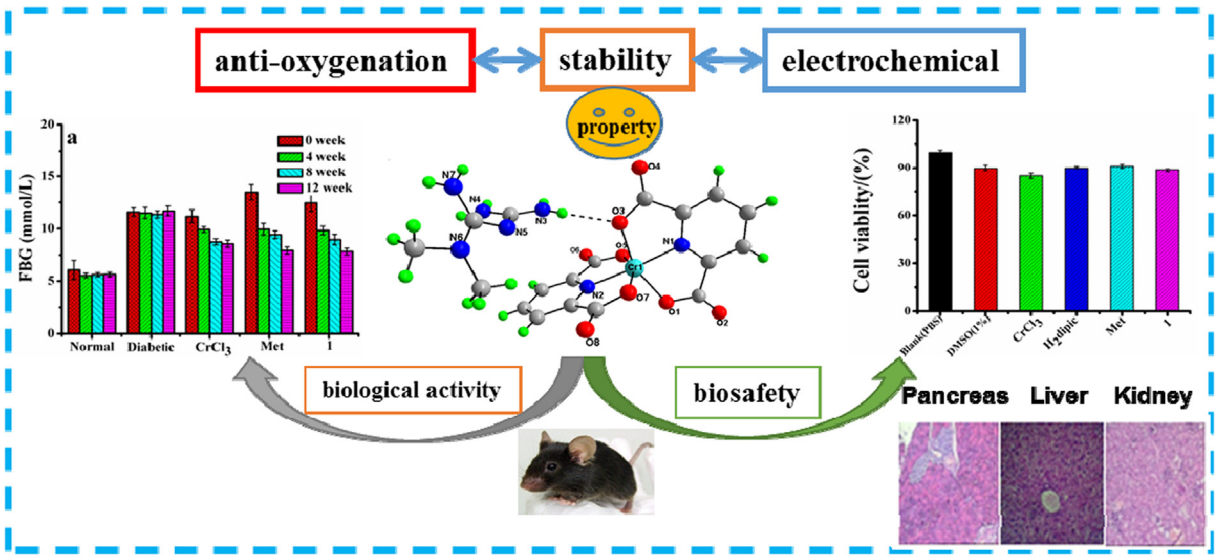

Fig. 1 Bioactivity and toxicity evaluation of complex ***1*** in T2DM C57BL/6 mice.

AG of Germany). Elements C, H and N were obtained on the *EURO* EA 3000 elemental analyser (Euro Vector of Italy). The IR spectra in the 4000–400 cm^{-1} were determined on the *Nicolet* iS5 spectrometer (Thermo Nicolet Corporation of America) by dispersing samples in the KBr disk. UV–Vis absorption spectra were recorded using the *Hitachi* UH-4150 spectrometer (Hitachi Company of Japan), and the fluorescence spectroscopy was conducted on the *Hitachi* F-7000 fluorescence spectrometer (Hitachi Company of Japan) at room temperature. The thermogravimetry (TG) analysis was carried out under nitrogen conditions on the *Netzsch* U-4100STA 2500 Regulus instrument (Netzsch Germany) at a heating rate of 20 °C·min^{-1} from 25 °C to 800 °C. The scanning electron microscopy (SEM) image was obtained using the *Zeiss EVO* MA10 electron microscope at an acceleration voltage of 30 kV. The XRD pattern of the sample was recorded on the *Bruker* D8-ADVANCE X-ray diffractometer (Bruker AG of Germany). All diffraction patterns were obtained with the Cu Kα radiation (λ = 1.5418 Å) by using a graphite monochromator at a scanning rate of 10° per minute. All biochemical indicators were measured on the *Beckman* AU5800 automatic biochemical analyser (Beckman Corporation of America).

2.3. Ethical approval

The animal experiment study was performed in the Animal Centre of First Hospital of Shanxi Medical University, which approved the animal experimental protocols with the qualified number SCXK (JIN) 2019–0001.

2.4. Synthesis and characterisation of complex 1

The $CrCl_3·6H_2O$ (2.665 g, 10 mmol) methanol solution (50 mL) was added dropwise into a 200 mL three-necked flask containing Met·HCl (1.666 g, 10 mmol) methanol solution (100 mL), NaOH (0.040 g, 10 mmol) and H_2dipic (3.310 g, 20 mmol). The mixture was stirred at 28 °C ± 3 °C in a water bath for 30 min, during which a deep purple solution was formed. The purple crystals suitable for X-ray structural analysis were obtained through the slow evaporation of the solvent at room temperature(Wang and Yao, 2009). Yield, 3.02 g (59%). EA for $Cr(C_7H_3NO_4)_2·C_4H_{12}N_5$, Calcd. (%): C 42.19, H 3.54, N 19.14; Found (%): C 41.97, H 3.62, N 19.05. Selected IR data (KBr pellet, cm^{-1}): 3424 (s), 3344 (s), 3240 (s), 3085 (w), 3056 (w), 1677 (Vs), 1643 (m), 1568 (s), 1505 (m), 1418 (m), 1323 (Vs), 1164 (s), 1087 (s), 917 (s), 772 (m), 746 (s), 697 (w), 681 (m), 596 (m), 451 (s) (**Figure S2**).

2.5. X-ray crystallographic analysis

The single crystal structure of (HMet)[Cr(dipic)$_2$] was obtained using the single-crystal X-ray diffraction technique. In all cases, intensity data were measured using the thin-slice × or ω- and ω-scans. The data for the complex were collected on the Siemens (Bruker) SMART CCD diffractometer by using monochromated Mo–*K*a radiation (0.71073 Å) at 293 K. The structure was solved using direct methods and refined using the least-squares method in the SHELXTL-97 program package (Sun et al., 1999). Absorption corrections were carried out using the SADABS program supplied by Bruker (Clodfelder et al., 2005). After all nonhydrogen atoms were refined anisotropically, the hydrogen atom attached to N and O atoms was located from different Fourier maps (O–H and N–H were fixed to 0.85 and 0.87 Å, respectively, later), and the remaining H atoms were placed in a calculated position with C–H = 0.95 and 0.98 Å for methyl groups. All hydrogen atoms were refined using a riding model with Uiso (H) = 1.2 Ueq (C, N) and 1.5 eq (C-methyl, O). Outlier reflections were omitted during the final refinement. The details of the crystallographic data collection, structural determination and refinement are summarised in Table 1. Selected bond lengths and angles of complex were presented in Table 2.

2.6. Density functional theoretical (DFT) computation

DFT computations were performed at the B3LYP/N,H,O,C/6–31 + G(d,p)/Cr/lanl2dz level to derive the optimised

Table 1 Crystal data and structure refinement of complex ***1***.

Complex	1
Formula	C18 H18 Cr N7 O8
Crystal system	Monoclinic
Space group	P2(1)/n
Formula weight	512.39
a (Å)	7.9044(6)
b (Å)	12.0899(11)
c (Å)	22.444(2)
α (°)	90.00
β (°)	90.7280(10)
γ (°)	90.00
V (Å^3)	2144.6(3)
Z	4
T (K)	298(2)
λ (Å)	0.71073
ρ (g·cm^{-3})	1.587
F(000)	1052
Theta range for data collection	2.48–25.02
Goodness-of-fit on F^2	0.971
R_1 [$I > 2\sigma(I)$][a]	0.0642
R_1 (all data)[a]	0.1336
wR_2 [$I > 2\sigma(I)$]	0.1435
wR_2 (all data)	0.1777

[a] $R = \sum(|F_o\text{-}F_c|)/\sum|F_o|$. $wR = \{\sum[w(|F_o\text{-}F_c|)^2]/\sum[w|Fo|^2]\}^{1/2}$.

geometry of normal modes of (HMet)[Cr(dipic)$_2$] by using the Gaussian 09 package (Ray, 1961). The molecular geometry was fully optimised using the Berny's optimisation algorithm, and its optimised structure was confirmed to have the lowest potential energy surface and highest thermodynamic stability.

2.7. Biochemical activity

Healthy C57BL/6 mice (number, 55; age, 50 days; body mass, 19–25 g) were purchased from the Licensed Laboratory of the Animal Breeding Center in Shanxi Medical University with the qualified number SCXK (JIN) 2019–0001. After being sent to an animal care facility, the mice were kept in a pathogen-free environment with controlled temperature (25 ± 3 °C) and humidity (55%–60%) and a 12/12 h (day/night) cycle during the whole experiment. After a week of adjustment period, the mice were kept in separate metal-free cages and fed semi-finished food. Control or high-fat (HF) diets composed of 51.5% ordinary feed, 10% soybean oil, 20% sucrose, 15% lard and 3.5% cholesterol. Mice had free access to food and clean water. The food intake was monitored daily, and the body mass gain was recorded weekly. After 30 days of feeding with these diets, mice were intraperitoneally injected with STZ (50 mg•kg^{-1} body mass in citric acid buffer, pH = 4.4) and continued feeding the HF diet for 30 days to induce diabetes, whereas the rest of mice (control group) were injected only with the carrier (citric buffer). Then, mice were starved for 16 h before treatment but were free to drink water. Blood samples were collected from the tail vein of the mice. After the STZ injection, at BG levels $\geq$ 11.1 mmol·L^{-1}, all the mice met the requirements of hyperglycemia model.

A total of 55 experimental mice were randomly divided into 1 normal and 4 diabetic groups (HF/STZ-induced diabetic mice) with 11 mice in each diabetic group. All mice had free access to standard solid food and drinking water. Drugs were administered at 1.0 mg Cr per kg body weigth (BW) orally once daily for 12 successive weeks (See TABLE S2), and the BW, fasting blood– glucose (FBG), fasting insulin (FINS), total cholesterol (TC), triglycerides (TG), high density lipoprotein (HDL) and low density lipoprotein (LDL) levels of the mice were tested every four weeks thereafter. All mice were fasted for 12–16 h, and their blood was collected from tail snips into capillary. After blood collection, 0.5 mg·mL^{-1} heparin and 10 mg·mL^{-1} NaF were added immediately. Next, the blood samples were centrifuged immediately and measured using the AU5800 Beckman automatic biochemical analyser.

2.8. In vitro cell viability/cytotoxicity study

The effects of $CrCl_3$, H_2dipic, Met and complex ***1*** on the viability of MCF-7 cancer cells were detected using the MTT assay (Sheldrick, 2008). Cells were diluted with medium to 2.5 × 10^4 cells per well, and aliquots (5 × 10^3 cells per 200 μL) were seeded in 96-well plates. After 14 h, cells were treated with $CrCl_3$, H_2dipic, Met and complex ***1*** (20 μL, 1 × 10^{-4} mol·L^{-1}, dimethyl sulfoxide (DMSO)/buffer, 1 : 9 *v*/*v*) and incubated for 24 h. Then, MTT (5 mg·mL^{-1}) was placed in 37.0 °C ± 0.5 °C DMEM and incubated in an environment maintained at 5% CO_2/95% air and 99% relative humidity for 4 h. The MTT culture medium was removed, and the formazan product was dissolved in DMSO (200 μL). The optical density of each hole was measured at 490 nm after the plates were oscillated for 15 min. Results showed a

Table 2 Selected bond distances (Å) and angles (°) for complex ***1***.

Bond distances					
Cr(1)-N(2)	1.961(4)	Cr(1)-O(5)	1.964(3)	Cr(1)-N(1)	1.969(4)
Cr(1)-O(3)	1.977(3)	Cr(1)-O(1)	1.982(4)	Cr(1)-O(7)	1.991(3)
N1-C2	1.324(6)	N1-C6	1.326(6)	N2-C9	1.316(6)
N2-C13	1.327(6)	N3-C15	1.320(7)	N4-C15	1.318(7)
N5-C15	1.317(6)	N5-C16	1.324(7)	N6-C16	1.334(6)
N6-C17	1.425(7)	N6-C18	1.455(7)	N7-C16	1.318(6)
Bond angles					
N(2)-Cr(1)-O(5)	78.87(15)	N(2)-Cr(1)- N(1)	175.85(17)	O(5)-Cr(1)-N(1)	100.08(15)
N(2)-Cr(1)-O(3)	97.29(15)	O(5)-Cr(1)-O(3)	92.48(14)	N(1)-Cr(1)-O(3)	78.71(16)
N(2)-Cr(1)-O(1)	105.52(15)	O(5)-Cr(1)-O(1)	91.91(15)	N(1)-Cr(1)-O(1)	78.48(16)
O(3)-Cr(1)-O(1)	157.19(15)	N(2)-Cr(1)-O(7)	78.52(15)	O(5)-Cr(1)-O(7)	157.35(15)
N(1)-Cr(1)-O(7)	102.57(15)	O(3)-Cr(1)-O(7)	91.79(14)	O(1)-Cr(1)-O(7)	92.73(15)

percentage of live cells relative to the untreated control group. Values are presented as mean ± standard deviation (SD) of three separate experiments carried out in sextuplicate.

2.9. Acute toxicity test

Healthy hermaphrodite C57BL/6 mice weighing 20–25 g were divided into four groups in this study. Saline was used as control, and $CrCl_3$, Met and complex ***1*** were used in the treatment groups. The mice were treated orally with dose of 10.0 g Cr per kg BW after fasting for 16 h. The behaviour of the mice was observed continuously for 1 h and within 24 h intermittently every 4 h. The intragastric administration for six days of feeding with the same dosage as administered orally. During the acute toxicity test, all mice had free access to drinking water and food. Mice were maintained at 25 °C (±2 °C) and about 50%–60% relative humidity throughout the experiment. Poisoning symptoms and deaths of all mice were observed for a week, and their weights were recorded at days 0, 3 and 7.

After 12 h of starvation, all mice were sacrificed by CO_2 at the end of the experiment. Subsequently, their pancreas, liver and kidney tissues were quickly excised, washed with saline and dried. According to previous research, these tissue structures were subjected to analyses. All animal experiments were conducted in accordance with local ethics committees.

2.10. Statistical analysis

Data were processed using the statistical SPSS software version 16.0 (SPSS Inc., Chicago, USA) and presented as mean ± SD. ANOVA and appropriate postmortem tests were used to determine whether the differences amongst groups were statistically significant. $P \leq 0.05$ was considered statistically significant.

3. Results and discussion

3.1. Synthesis and characterisation of complex 1

In terms of preparation, the reaction of $CrCl_3{\cdot}6H_2O$ with H_2-dipic and Met in MeOH–H_2O solution (Scheme 1) was carried out at room temperature, and the purple crystals were obtained by slow evaporation of the solvent at ambient temperature. The X-ray crystal structure diffraction suggested that the molecular formula of complex ***1*** was (HMet)[Cr(dipic)$_2$], which was consistent with the elemental analysis and spectral analysis data. Complex ***1*** was soluble in DMF and DMSO and dissolved partially in H_2O and CH_3OH.

The infrared (IR) absorption spectroscopy is one of the important methods for the determination of the chelation reaction. In the IR spectrum of H_2dipic and complex ***1*** (**Figure S2**), the aromatic CHs of pyridine and the N–H stretching vibrations of Met appeared on the 3424–3056 cm^{-1} region (Sheldrick, 1996). In addition, the sharp and strong peaks at 1677 and 1323 cm^{-1} corresponded to the asymmetric and symmetric stretching, respectively, of $-COO^-$ groups. The value of $\Delta(\nu_{as} - \nu_s)$ was 254 cm^{-1} (>200 cm^{-1}), indicating the monochelation of the $-COO^-$ group to the metal ion (Frisch et al., 2013). Moreover; by comparing the IR images of ligand, it can be seen that there is no characteristic peak of free carboxyl groups near 3550 and 1700 cm^{-1} of the complex ***1***, indicating that all carboxyl groups in the ligand are ionized and participate in the coordination. This finding was consistent with the results of the X-ray crystal analysis. Moreover, a specific absorption band near 451 cm^{-1} with two shoulders could be attributed to the ν(Cr–N) and the ν(Cr–O) stretching vibrations (Mosmann, 1983).

The UV–vis spectra of Met, H_2dipic, $CrCl_3$ and complex ***1*** are obtained with DMSO at room temperature (**Figure S3a**). In the Met, H_2dipic and complex ***1***, the UV region peaks corresponding to the $\pi \rightarrow \pi^*$ transitions were observed at 238, 270 and 262 nm, respectively. Compared with the H_2dipic ligand, an 8 nm blue shift was observed in complex ***1***. Two wide absorption bands located at about 430 and 607 nm for $CrCl_3$ and 352 and 550 nm for the complex ***1*** with strong blue shifts corresponded to the *d–d* transitions of Cr(III) ions (Mosmann, 1983; Bellamy, 1975; Nakamoto, 1997); and the two bands indicated the pseudo-octahedral configuration around the Cr (III) ion (González-Baró et al., 2008; Rastegarnia et al., 2020). The hypochromatic shifts of $\pi \rightarrow \pi^*$ and the *d–d* transitions in complex ***1*** were due to the coordination of chromium with N and O of H_2dipic, and electron clouds were redistributed in the original H_2dipic (Eshtiagh-Hosseini et al., 2010; Mosmann, 1983).

Figure S3b displays relatively strong fluorescence intensity of the free H_2dipic in DMSO, λ_{ex} = 300 nm, with a maximum emission of around 400 nm (curve b). After coordination with Cr(III), the fluorescence was quenched completely at 400 nm. The title complex had little fluorescence in DMSO, as shown in **Figure S3b** (curve a). As shown in **Figure S4**, the initial decomposition temperature of the complex was over 289 °C, indicating good thermostability of complex ***1***. The framework of the complex was not easily broken.

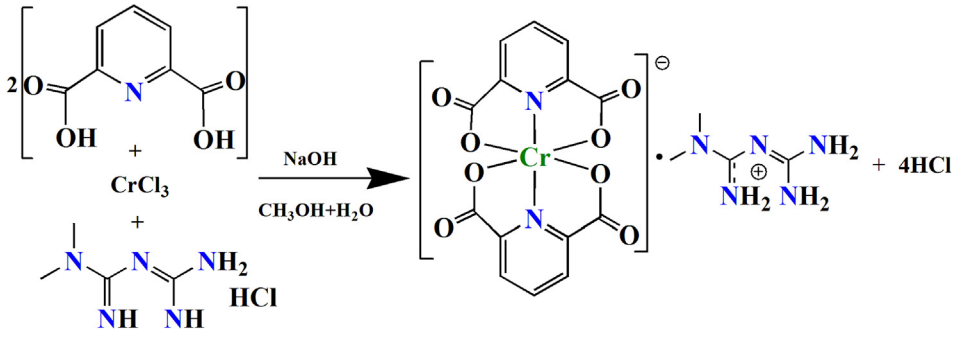

Scheme 1 Schematic route of the synthesis of complex ***1***.

3.2. Structure of complex 1

The asymmetric unit of (HMet)[Cr(dipic)$_2$] was composed of [Cr(dipic)$_2$]$^-$ and HMet$^+$ as counter ion (Fig. 2**a**). The two dipic ligands were coordinated to one chromium atom in a tridentate way, forming a twisted octahedral coordination environment consisting of 4O atoms and 2 N atoms. Furthermore, Fig. 2**b** shows the optimised molecule structure with the B3LYP calculations, and the same crystal structure of complex ***1*** was obtained using X-ray crystallography studies. The values of Cr–N bond distances were 1.961(4) and 1.969(4) Å, and the Cr(1)–O bond distances were 1.964(3), 1.977(3), 1.982(4) and 1.991(3) Å (average = 1.978 Å). All bond lengths were the same as those of the related structures (Öztirk et al., 2006). The junction of the metal ion was close to the intersection of the coordination planes (along the N1···N2 direction). The main bond lengths and angles of (HMet)(Cr[dipic]$_2$) are listed in Table 2. The calculated and the experimental results for complex ***1*** agreed well (**Table S1**). Met was protonated as a counter ion to balance the [Cr(dipic)$_2$]$^-$. The C–N bonds of the biguanidium moiety ranged from 1.317(6) to 1.455(7) Å in the cation (Table 2) and were consistent with that in literature (Dong et al., 2016).

The hydrogen bond geometry of the complex is listed in Table 3 and illustrated in Fig. 2**c**. A large number of intramolecular and intermolecular hydrogen bonds strengthened the crystal structure of the compound. The intermolecular hydrogen bonding was formed between the biguanidium groups and the carboxylate groups of the dipic. These intermolecular hydrogen bonds could enhance the stability of the complex ***1***, which corresponded to the result of the TG analysis.

3.3. Stability of the complex in solution

The stability of complex ***1*** in solution was first studied at different temperatures for 15 min by using UV–vis spectroscopy to explore the biological activity of complex ***1***. As shown in **Figure S5a**, the absorption peak of complex ***1*** had almost no displacement in the UV range, whereas in the visible region,

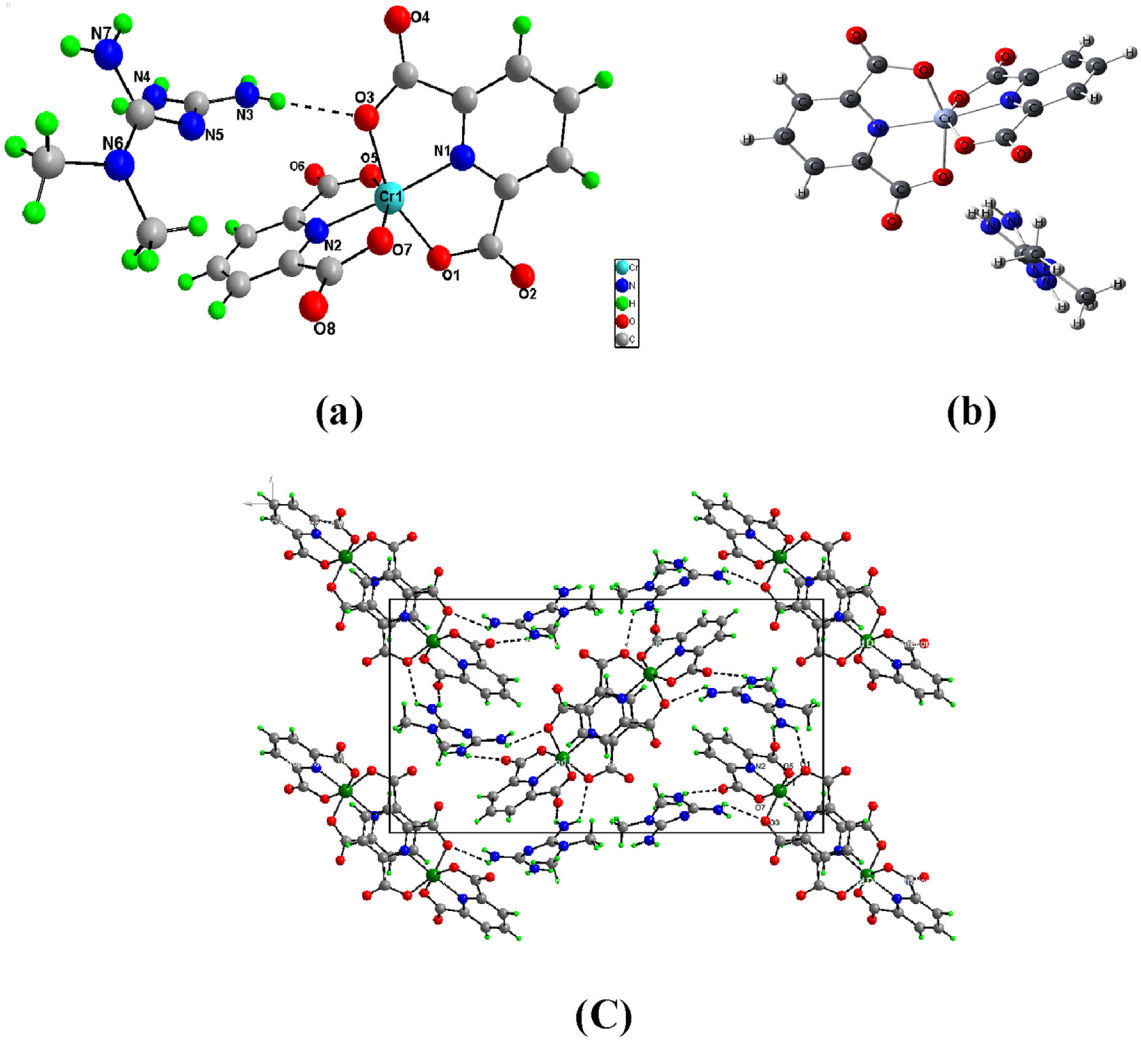

Fig. 2 **(a)** The crystal structure of complex ***1***. Dashed lines indicate hydrogen bonds within asymmetric unit. **(b)** Optimized structure of the [Cr(dipic)$_2$]$^-$ as anionic complex and free [HMet]$^+$ ligand with atom numbering. **(c)** The intermolecular hydrogen bonds between the biguanidium groups and the carboxylate groups of the dipic.

Table 3 Hydrogen bond details, distances (Å) and angles (°) for complex ***1***.

D – H...A	D–H	H...A	D...A	D–H...A
N7 – H7B ... O1	0.86	2.42	2.980(6)	123.7
N7 – H7A ... O6	0.86	2.06	2.823(6)	148.1
N4 – H4B ... O8	0.86	2.32	3.063(6)	145.1
N4 – H4A ... O2	0.86	2.20	2.992(6)	154.1
N3 – H3B ... O8	0.86	2.06	2.867(6)	156.7
N3 – H3A ... O3	0.86	2.14	2.951(6)	156.2

the *d–d* transition began to disappear slowly above 37 °C, indicating that the complex solution should be kept below 37 °C.

The Cr(VI) can induce genotoxicity or carcinogenicity (Hamada et al., 2003; Adam et al., 2015), and growing evidence shows that Cr(III) complexes are partially oxidised to carcinogenic Cr(VI) and Cr(V) in *vivo* (Aghabozorg et al., ; Aghabozorg et al., 2008; Dong et al.,). The oxidation of complex ***1*** by H_2O_2 in phosphatic buffer solution (PBS), DMEM and HSA medium solutions were examined using the UV–vis spectroscopy at 37 °C and physiological pH (7.4) to explore the antioxygenation potential of the complex. The results of the oxidation reaction are displayed in **Figure S5b**, and the inset that has appeared at 548 nm reflects the generation of Cr(VI) in different solutions. As demonstrated in **Figure S5b**, the complex ***1*** generated more Cr(VI) in DMEM and HSA mediums than in the PBS buffer, which might be due to the competitive effect of protein and other small molecules on Cr(III), which accelerated the release rate of the complex and made it easy to be oxidized, and that was consistent with the results of similar studies (Dong et al., ; Codd et al., 2001). In addition, because Australia inorganic biology Professor Lay has proposed the chromium(III) hypoglycaemic action mechanism under physiological conditions Cr(III) by H_2O_2 or ClO^- oxidised to Cr(VI), and then the dithiothreitol (DTT) under the action of reducing agent to inhibit protein tyrosine phosphate the activity of lipase (PTPs) or prevents its expression, thus infer that Cr (III) the antidiabetic properties may be related to Cr(VI) ions have indirect relationship (Aghabozorg et al., ; Aghabozorg et al., 2008). This findings is consistent with the results of Professor Lay's experiment [**47b**].

3.4. Electrochemical property

The biotoxicity of the Cr(III) complex may be reduced by shifting the reduction potentials and conferring reversibility of the redox couples. The electrochemical property of complex ***1*** was also investigated through cyclic voltammetry (CV) by using the saturated calomel electrode (SCE) as a reference electrode. The electrochemical experiment was conducted on 1.0 mM complex ***1*** in DMSO under nitrogen atmosphere, and tetrabutylammonium perchlorate (0.10 M) was used as a supporting electrolyte. The CV curve is presented in **Figure S6**. As shown in the voltammogram of complex ***1***, the oxidation peak was approximately + 1.25 eV, which could be assigned to the Cr(V)/Cr(III) redox process (Levina and Lay, 2008). Another redox couples occurred at E_{re} = − 1.24 (vs. SCE), and E_{ox} = − 1.18 V (vs. SCE) was due to the quasireversible Cr(III)/Cr(II) redox process. The $E_{1/2}$ values for Cr(II)/Cr(I) couple were − 1.70/−1.61 V (Wu et al., 2016). In addition, the electrochemical signals of the ligand in DMSO were not observed under the same conditions.

3.5. SEM and XRD

The surface morphology of complex ***1*** was determined using SEM (**Figure S7a**). The SEM micrograph revealed clear large grains with variant grain sizes. The XRD patterns in the range of $5° < 2\theta < 80°$ of complex ***1*** was done. The diffraction pattern of the collected complex is shown in **Figure S7b**. The XRD patterns refer to the crystalline properties for complex ***1***. The variation in the Cr(III) complex diffraction pattern can be attributed to the formation of a new structure (Rastegarnia et al., 2020). The SEM images and the XRD patterns show that the crystal shape of complex ***1*** was intact, and the crystallinity was good.

3.6. HOMO–LUMO analysis

On the basis of the DFT and using a repeat unit as a model, the geometric configuration and the electron density distributions of the LUMO and the HOMO energy levels of complex ***1*** were obtained (**Figure S8**). From the DFT calculations, the HOMO energy level of the complex was − 6.05 eV, and the electron density was distributed on the CrN_2O_4 moiety. The LUMO energy level of complex ***1*** was − 3.16 eV, and the electron density was distributed on two dipic ring moieties. The HOMO → LUMO transition implied that the electron density cloud transferred from the CrN_2O_4 to the dipic ring. The energy band gap (ΔE) between the HOMO and the LUMO of the molecule was about 2.89 eV. A large HOMO–LUMO gap indicates good kinetic stability and low reactivity because adding electrons to a high-lying LUMO or extracting them from a low-lying HOMO is energy unfriendly (Levina and Lay, 2005). This large energy gap can also demonstrate the blue shift of the complex ***1*** in the electron absorption spectrum (Eshtiagh-Hosseini et al., 2010; Mosmann, 1983).

3.7. Bioactivity evaluation

The primary bioactivity of complex ***1*** on the STZ mice was examined for 12 weeks to assess the therapeutic effects of synthetic complex ***1*** on T2DM. As shown in **Figure S9 and** Table 4, all indexes of diabetic mice were significantly higher than those of the normal group except body weight. Significant improvements in all indicators occurred in the intervention groups compared with the diabetes group. No significant change was observed in the physical activity during the drug intervention, and almost all mice survived. Details are as follows.

In **Figure S9a**, the recommended dose of STZ significantly increased the FBG levels. The changes in the FBG levels in the $CrCl_3$, Met and complex ***1*** during the 4, 8 and 12 weeks of intragastric administration were monitored in normal and STZ mice, as shown in **Figure S9a**. Overall, after administration with $CrCl_3$, Met and complex ***1*** for 4, 8 and 12 weeks, the FBG levels of diabetic mice decreased significantly ($P < 0.05$) compared with those of the control group. Clearly, ***1*** for 4, 8 and 12 weeks, the glucose-lowering rates of $CrCl_3$ were 11.25%, 20.93% and 23.43%, respectively; those of Met were 26.13%, 30.07% and 41.20%, respectively; and those of the complex were 21.04%, 28.03% and 37.18%, respectively. Census figures indicate the following. 1) Compared with the Cr(III) complexes group, diabetic mice still experienced a significant decrease in blood glucose levels after receiving Met. 2) The $CrCl_3$-treated group elicited a slight decrease in BG levels compared with the organic Cr(III) complex combination group, which might be the related to the Cr(III) absorption. Besides, results suggested that the complex ***1*** had a potential FBG reduction effect equivalent to the Met. Experimental results are also similar to those reported by El–Megharbel (Headlam and Lay, 2016).

Next, the insulin is the main hormone that regulates glucose metabolism and is overexpressed in patients with T2DM, leading to insulin resistance. As shown in **Figure S9b**, untreated groups had significantly higher FINS levels versus the normal control group, and the $CrCl_3$-, Met- and complex ***1***-treated groups had slightly lower FINS levels versus the control group. Thus far, the expected insulin levels were unclear, but the FINS levels for the $CrCl_3$-, Met- and complex ***1***-supplemented groups at 12 weeks decreased. This result further demonstrated that the complex ***1*** could improve the insulin resistance caused by T2DM and effectively alleviate major syndromes.

Cardiovascular diseases and diabetes are associated with hyperlipidaemia (Forslund et al., 2015). Thus, the serum lipid and lipoprotein levels in normal and diabetic mice were also investigated after 4, 8 and 12 weeks of STZ-induced diabetes. These results are described in **Figures S9c and S9d**. Overall, all treated groups exhibited alleviated TC and TG levels compared with the diabetic control group. As demonstrated in **Figures S9c and S9d**, compared with the diabetic control group, the TC and the TG levels decreased significantly ($P < 0.05$) when the mice were treated by $CrCl_3$, Met and complex ***1***. After supplementation of complex ***1*** for 12 weeks, the reduction percentage of TC and TG levels in the complex ***1*** group were about 35.28% and 32.40%, respectively, indicating better effect than those in the $CrCl_3$ and Met groups. Results showed that complex ***1*** had considerable ability in modulating lipid levels and decreasing the fatty acid properties of Cr(III), which were consistent with literature reports (Vincent, 2015; Liu et al., 2015; Preuss et al., 2008; Kim et al., 2004). This result could be due to the synergistic effect of Cr(III), dipic and Met in complex ***1***.

In addition, the HDL-c and the LDL-c levels of STZ mice were tested for 12 weeks. As shown in **Figures S9e and S9f**, the

Table 4 Alters of BW, FBG, FINS, TC, TG, HDL and LDL levels of control group and the mice followed administration with $CrCl_3$, Met and complex ***1*** carrier (control) by oral gavage during biochemical activity study.

	week	Normal	Diabetic	$CrCl_3$-treated	Met-treated	1-treated
BM/g	0	19.24 ± 1.16	23.62 ± 2.05	24.14 ± 2.14	21.59 ± 2.93	22.92 ± 1.86
	4	22.45 ± 1.55	30.5 ± 2.40	29.42 ± 1.62	28.64 ± 0.82	29.28 ± 1.86
	8	29.35 ± 1.48	40.82 ± 2.18	37.89 ± 3.01	37.28 ± 2.63	39.17 ± 1.77
	12	32.26 ± 1.28	48.26 ± 3.00	44.94 ± 3.01	43.08 ± 3.11	46.64 ± 1.73
FBG	0	6.07 ± 0.32	11.59 ± 0.39$^{\#}$	11.18 ± 0.61$^{\#}$	13.47 ± 0.57$^{\#}$	12.45 ± 0.62$^{\#}$
/mmol•L^{-1}	4	5.54 ± 0.23	11.50 ± 0.52$^{\#}$	9.92 ± 0.28$^{\#*}$	9.95 ± 0.52$^{\#*}$	9.83 ± 0.40$^{\#*}$
	8	5.60 ± 0.20	11.37 ± 0.35$^{\#}$	8.84 ± 0.30$^{\#*}$	9.42 ± 0.38$^{\#*}$	8.96 ± 0.51$^{\#*}$
	12	5.64 ± 0.21	11.70 ± 0.58$^{\#}$	8.56 ± 0.35$^{\#*}$	7.92 ± 0.34$^{\#*}$	7.82 ± 0.34$^{\#*}$
FINS	0	12.36 ± 1.50	19.13 ± 1.21$^{\#}$	19.80 ± 0.54$^{\#}$	18.78 ± 1.60$^{\#}$	19.97 ± 0.67$^{\#}$
/mmol•L^{-1}	4	11.49 ± 0.52	21.71 ± 0.52$^{\#}$	17.23 ± 0.91$^{\#*}$	19.64 ± 0.58$^{\#}$	18.22 ± 0.65$^{\#*}$
	8	11.25 ± 0.34	21.11 ± 0.66$^{\#}$	17.22 ± 0.86$^{\#*}$	18.40 ± 0.58$^{\#*}$	17.20 ± 0.54$^{\#*}$
	12	11.55 ± 0.38	19.89 ± 0.46$^{\#}$	15.99 ± 0.76$^{\#*}$	14.87 ± 0.72$^{\#*}$	15.28 ± 0.59$^{\#*}$
TC	0	1.92 ± 0.15	4.66 ± 0.64$^{\#}$	4.28 ± 0.32$^{\#}$	4.41 ± 0.74$^{\#}$	4.45 ± 0.34$^{\#}$
/mmol•L^{-1}	4	1.74 ± 0.12	4.17 ± 0.32$^{\#}$	3.77 ± 0.19$^{\#*}$	3.90 ± 0.26$^{\#}$	3.34 ± 0.20$^{\#*}$
	8	1.92 ± 0.093	4.68 ± 0.23$^{\#}$	3.50 ± 0.24$^{\#*}$	3.68 ± 0.20$^{\#*}$	3.08 ± 0.19$^{\#*}$
	12	1.95 ± 0.083	4.14 ± 0.24$^{\#}$	3.66 ± 0.28$^{\#*}$	3.51 ± 0.20$^{\#*}$	2.88 ± 0.22$^{\#*}$
TG	0	0.55 ± 0.050	1.63 ± 0.22$^{\#}$	2.02 ± 0.19$^{\#}$	1.77 ± 0.22$^{\#}$	1.79 ± 0.12$^{\#}$
/mmol•L^{-1}	4	0.50 ± 0.043	1.92 ± 0.21$^{\#}$	1.87 ± 0.20$^{\#*}$	1.70 ± 0.22$^{\#*}$	1.49 ± 0.11$^{\#*}$
	8	0.52 ± 0.026	2.04 ± 0.21$^{\#}$	1.63 ± 0.14$^{\#*}$	1.72 ± 0.11$^{\#*}$	1.29 ± 0.12$^{\#*}$
	12	0.53 ± 0.029	2.41 ± 0.23$^{\#}$	1.69 ± 0.24$^{\#*}$	1.67 ± 0.15$^{\#*}$	1.21 ± 0.13$^{\#*}$
HDL	0	1.31 ± 0.09	0.90 ± 0.099$^{\#}$	0.87 ± 0.062$^{\#}$	0.82 ± 0.070$^{\#}$	0.91 ± 0.07$^{\#}$
/mmol•L^{-1}	4	1.24 ± 0.092	0.80 ± 0.064$^{\#}$	0.98 ± 0.059$^{\#}$	0.86 ± 0.081$^{\#}$	0.96 ± 0.053$^{\#*}$
	8	1.19 ± 0.086	0.75 ± 0.040$^{\#}$	0.86 ± 0.049$^{\#}$	0.86 ± 0.080$^{\#}$	0.89 ± 0.056$^{\#}$
	12	1.21 ± 0.081	0.79 ± 0.033$^{\#}$	0.90 ± 0.050$^{\#}$	0.84 ± 0.080$^{\#}$	0.94 ± 0.052$^{\#}$
LDL	0	0.75 ± 0.064	0.87 ± 0.050$^{\#}$	0.85 ± 0.095$^{\#}$	0.80 ± 0.061	1.02 ± 0.06$^{\#}$
/mmol•L^{-1}	4	0.68 ± 0.027	0.99 ± 0.064$^{\#}$	0.76 ± 0.052*	0.81 ± 0.050*	0.83 ± 0.053$^{\#*}$
	8	0.70 ± 0.024	1.09 ± 0.062$^{\#}$	0.81 ± 0.066*	0.81 ± 0.050*	0.81 ± 0.05*
	12	0.71 ± 0.028	0.99 ± 0.054$^{\#}$	0.84 ± 0.040$^{\#}$	0.8 ± 0.036$^{\#*}$	0.80 ± 0.034*

#: diabetic group versus normal control ($p < 0.05$). *: intervention group versus diabetic group ($p < 0.05$).

HDL-c and the LDL levels of the entire experimental group had a slight variation throughout the intervention, and further experiments were needed to test irregular changes. Overall, the improvements in lipid and lipoprotein levels suggested that the complex ***1*** was another promising candidate for regulating lipid metabolism in T2DM mice, and this result was in accordance with relevant literature reports (Chai et al., 2017; Stout et al., 2009;Li et al., 2012; Wang et al., 2017).

In conclusion, the results of biological activity evaluation agree with the reported studies, which show that Met and chromium inhibit hyperglycaemia and hyperlipidaemia (Li et al., 2012; Stout et al., 2009; Megharbel,; Wang et al., 2017). Hence, results correlate with a synergistic effect of Met, dipicolinic acid and chromium in its (HMet)[Cr(dipic)$_2$]-complex form.

3.8. MTT assay

The effect of complex ***1*** on cell viability was determined using the MTT assay and compared with $CrCl_3$, H_2dipic, Met and complex alone. Specifically, the growth of MCF-7 cells was measured for cytotoxicity, and the survival rate was tested after incubation with the complex for 24 h by using prior MTT treatment. Results are shown in Fig. 3, with DMSO (1%) as the control. Overall, no statistically significant difference was observed. The ability of cells to survive was about 85%, 90%, 91% and 89% for $CrCl_3$, H_2dipic, Met and complex ***1***, respectively, and the cell viability of all samples were all over 85%. This result indicated that the tested complex ***1*** was nearly nontoxic to cell lines within 24 h and probably possessed good biocompatibility (Dong et al., 2020; Kuskov et al., 2016). Moreover, the cytotoxicity of complex ***1*** in cells is a complicated process (Aghabozorg et al.,) and should be further noted that the cells are exposed to the intact complex ***1*** in *vitro*, which does not occur in human cells (Liu et al., 2016).

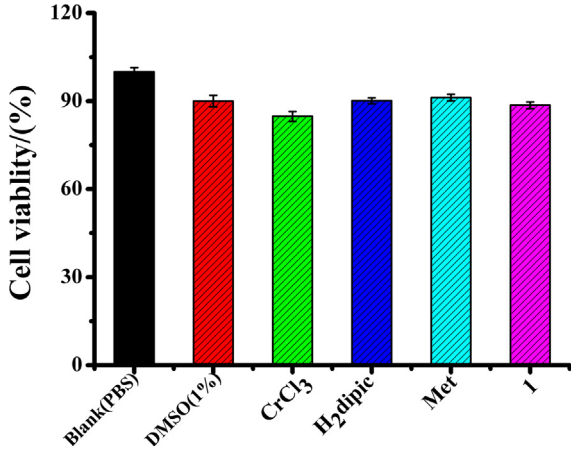

Fig. 3 Cytotoxic effect of complex ***1*** on cancer cell line. The cytotoxicity of $CrCl_3$, H_2dipic, Met and complex ***1*** (1.0×10^{-4} M) were evaluated on MCF–7 cell line (2.5×10^4 cells/mL) by the MTT assay for 24 h. 1% DMSO (V:V) was used as a control experiment. Results are mean ± SD of six independent experiments. There was no significant difference between the data ($P > 0.05$).

3.9. Acute toxicity

The complex ***1*** was used in the experimental group, and the $CrCl_3$ and the Met were used in the control group to further evaluate the acute toxicity of complex ***1*** in *vivo*. The histopathological changes in the pancreas, kidney and liver sections in C57 mice were observed after gavage of 10.0 g Cr per kg and 1% DMSO for seven days, as shown in Fig. 4. The mice were all alive during the experiment. No significant difference was observed in the weight between the experimental and the control groups (**Figure S10** and **Table S2**).

In Fig. 4, there were no significant changes in the histological morphology of the pancreas and kidneys of the mice in each group under the microscope. The histological sections of the pancreatic acinar and the ductal cells of the C57 rats in the experimental and the control groups were normal, and no oedema or inflammation was observed. The collection tubule shown here was normal. The complex ***1*** group of the pancreatic duct secreted protein fluid with normal structure. The liver histology of mice in the control and the treatment groups displayed normal lobular structure and normal hepatic spinal cord aggregation. Compared with the control group, the liver of some diabetic model mice was accompanied by mild edema and steatosis, which may be related to the high-sugar and high-fat diet. No morphological changes with significant pathological significance, such as fibrosis, necrosis, pseudolobules, and inflammation, were observed. In addition, the microanatomic structure, distal-collecting tubules and interstitial tissue of the kidney of C57 mice by gavage were normal without inflammation or interstitial fibrosis.

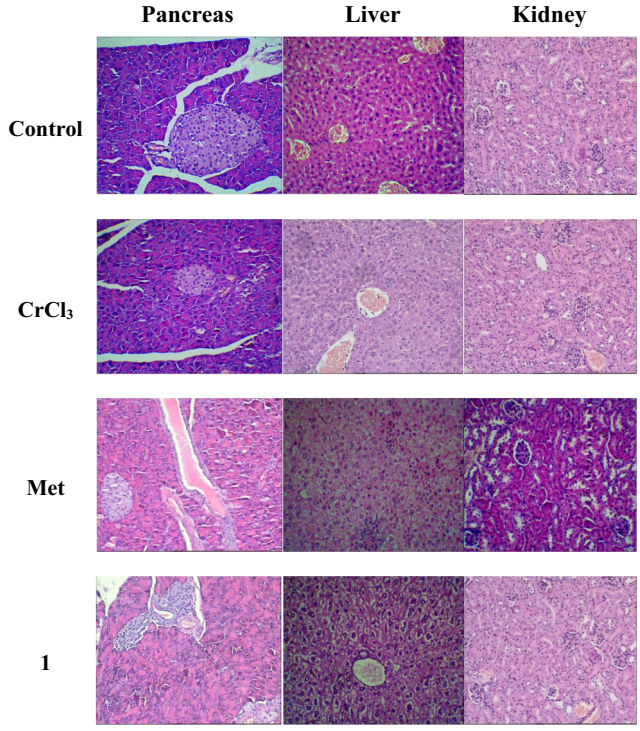

Fig. 4 Histopathological images of pancreas, liver and kidney sections treated $CrCl_3$, Met and complex ***1*** at dose 1.0 g Cr/kg BW.

In summary, no pathological change was observed in the pancreas, liver and kidney of all treated rats. This result was completely consistent with literature reports (Liu et al., 2016; Weeks et al., 2004; Huang et al., 2017; Mahmoud et al., 2016; Tang et al., 2015) and proved that the tested complex ***1*** exhibited low toxicity or nontoxicity to mice after a single high-dose drug intervention during this time.

4. Conclusions

In this paper, the structure, nature, biology and toxicology of metal–drug interactions of Cr(III) with dipic and Met drug have been studied in detail at ambient temperature. The structure of complex ***1*** has been fully characterised through physicochemical and spectroscopic techniques, and results are consistent with the molecular structure optimised by DFT. TG studies with decomposition temperature of 289 °C indicate its excellent stability. The preliminary results of biological activities demonstrate that the reduction percentage of TC and TG levels in the complex ***1*** group are about 35.28% and 32.40%, respectively, and has improved compared with those in the $CrCl_3$- and Met-treated groups, which may be due to synergies of Cr(III) with H_2dipic and Met. Furthermore, the acute oral toxicity tests confirm that the complex ***1*** has no lesion on liver, kidney and pancreas biopsy. The MTT assay also shows that the complex ***1*** exhibits low cytotoxicity and improved biocompatibility. Consequently, the prepared Cr (III) complex on the basis of H_2dipic and Met is nontoxic and has a potential for safe application as hypoglycaemic lipid-lowering drug. Further biological tests of complex ***1*** is in progress and reported subsequently.

Declaration of Competing Interest

The authors declare that they have no known competing financial interests or personal relationships that could have appeared to influence the work reported in this paper.

Acknowledgements

We are very grateful for financial support from the National Natural Science Foundation of PR China (No. 21571117, 21701121), the Natural Science Foundation of Shanxi Province (No. 201801D121064), the Science and Technology Innovation Project of Colleges and Universities in Shanxi Province (No. 2020L0585), and the Innovation Project for College Students in Shanxi Province (No. 2020491).

Appendix A. Supplementary data

Supplementary data to this article can be found online at https://doi.org/10.1016/j.arabjc.2021.103236.

References

Adam, A.M.A., Sharshar, T., Mohamed, M.A., Ibrahim, O.B., Refat, M.S., 2015. Study of chemical bonding, physical and biological effect of metformin drug as an organized medicine for diabetes patients with chromium(III) and vanadium(IV) ions. Spectrochim. Acta Part A Mol. Biomol. Spectrosc. 149, 323–332.

(a) H. Aghabozorg, Z. Derikvand, M.M. Olmstead, J.A. Gharamaleki, Creatininium bis(pyridine-2,6-dicarboxylato) chromate(III) pyridine-2,6-dicarboxylic acid hexahydrate, Acta Cryst. E, 2008, 64: m1234-1235;

H. Aghabozorg, F. Manteghi, S. Sheshmani, A brief review on structural concepts of novel supramolecular proton transfer compounds and their metal complexes, J. Iran Chem. Soc., 2008, 5: 184-227.

Aghabozorg, H., Roshan, L., Firoozi, N., Ghadermazi, M., Bagheri, S., 2008. 2,6-Diamino pyridinium bis(4-hydroxypyridine-2,6-dicarboxylato-κ^3O^2, N, O6)-chromate(III) dehydrate. Acta Cryst. E 64, m1208–1209.

Al-Saif, F.A., Refat, M.S., 2013. Synthesis, spectroscopic, and thermal investigation of transition and non-transition complexes of metformin as potential insulin-mimetic agents. J. Therm. Anal. Calorim. 111 (3), 2079–2096. https://doi.org/10.1007/s10973-012-2459-3.

Anderson, R.A., 2000. Chromium in the prevention and control of diabetes. Diab. Metab. 26, 22–27.

Bellamy, L.J., 1975. The infrared spectra of complex molecules. Chapman and Hall, London.

I.B. Sahra, Y.L. Marchand-Brustel, J.F. Tanti, F. Bost, Metformin in cancer therapy: a new perspective for an old antidiabetic drug? Mol. Cancer Ther., 2010, 9: 1092-1099.

F. Bentefrit, G. Morgant, B. Viossat, S. Leonce, N. Guilbaud, A. Pierre, G. Atassi, N.H. Dung, Synthesis and antitumor activity of the metformin platinum(IV) complex. Crystal structure of the tetrachloro (metformin) platinum(IV) dimethylsulfoxide solvate, J. Inorg. Biochem., 1997, 68: 53-59.

Cefalu, W.T., Hu, F.B., 2004. Role of Chromium in Human Health and in Diabetes. Diabetes Care 27 (11), 2741–2751.

Chai, J., Liu, Y., Dong, J., Liu, B., Yang, B., 2017. Synthesis, structure, chemical and bioactivity behavior of eight chromium(III) picolinate derivatives $Cr(R\text{-}pic)_3$. Inorg. Chim. Acta 466, 151–159.

Clodfelder, B.J., Gullick, B.M., Lukaski, H.C., Neggers, Y., Vincent, J.B., 2005. Oral administration of the biomimetic $[Cr_3O(O_2CCH_2CH_3)_6(H_2O)_3]^+$ increases insulin sensitivity and improves blood plasma variables in healthy and type 2 diabetic rats. J. Biol. Inorg. Chem. 10 (2), 119–130. https://doi.org/10.1007/s00775-004-0618-0.

Codd, R., Dillon, C.T., Levina, A., Lay, P.A., 2001. Studies on the genotoxicity of chromium: from the test tube to the cell. Coord. Chem. Rev. 216-217, 537–582.

Després, J.-P., Lemieux, I., 2006. Abdominal obesity and metabolic syndrome. Nature 444 (7121), 881–887.

Di Bona, K.R., Love, S., Rhodes, N.R., McAdory, DeAna, Sinha, S. H., Kern, N., Kent, J., Strickland, J., Wilson, A., Beaird, J., Ramage, J., Rasco, J.F., Vincent, J.B., 2011. Chromium is not an essential trace element for mammals: effects of a "low-chromium" diet. J. Biol. Inorg. Chem. 16 (3), 381–390. https://doi.org/10.1007/s00775-010-0734-y.

J.L. Dong, B. Liu, B.S. Yang, Crystal structure of bis{2-[amino-(iminiumyl)methyl] -1,1-dimethylguanidine} carbonate methanol disolvate, Acta Cryst. E, 2015, 71: o747-748.

Dong, J., Liu, B., Yang, B., 2016. Synthesis, crystal structure and magnetic properties of trinuclear chromium(III) basic carboxylate assembly: [Cr3O(salH)7(H2O)2] (salH2 = salicylic acid), a new member of [Cr3O] family. J. Mol. Struct. 1116, 311–316.

Dong, J., Shen, L., Wen, B., Song, Z., Feng, J., Liang, G., Liu, B., Yang, B., 2020. Synthesis of A Novel Anti-diabetes Chromium(III) Complex and Investigation of Its Biological Activity and Mechanism. Acta Chim. Sinica 78 (11), 1260. https://doi.org/10.6023/A20070285.

H. Eshtiagh-Hosseini, Z. Yousefi, M. Mirzaei, Y.G. Chen, S.A. Beyramabadi, A. Shokrollahi, R. Aghaei, A new supramolecular compound of chrome(III): synthesis, spectroscopic characterization, X-ray crystal structure, DFT, and solution studies, J. Mol. Struct., 2010, 973: 1-8.

Forslund, K., Hildebrand, F., Nielsen, T., Falony, G., Le Chatelier, E., Sunagawa, S., Prifti, E., Vieira-Silva, S., Gudmundsdottir, V., Krogh Pedersen, H., Arumugam, M., Kristiansen, K., Yvonne Voigt, A., Vestergaard, H., Hercog, R., Igor Costea, P., Roat Kultima, J., Li, J., Jørgensen, T., Levenez, F., Dore, J., Bjørn Nielsen, H., Brunak, S., Raes, J., Hansen, T., Wang, J., Dusko Ehrlich, S., Bork, P., Pedersen, O., 2015. Disentangling type 2 diabetes and metformin treatment signatures in the human gut microbiota. Nature 528 (7581), 262–266.

M.J. Frisch, G.W. Trucks, H.B Schlegel, Gaussian 09, Revision D.01, Gaussian Inc., Wallingford CT, 2013.

Ghasemi, K., Rezvani, A.R., Rosli, M.M., Abdul Razak, I., Moghimi, A., Ghasemi, F., 2014. Potential antidiabetic drug involving a zinc anionic complex of dipic and metformin as counter ions: Synthesis, characterization, crystal structure and electrochemical studies. J. Mol. Struct. 1074, 79–84.

A.C. González-Baró, R. Pis-Diez, O.E. Piro, B.S. Parajón-Costa, Crystal structures, theoretical calculations, spectroscopic and electrochemical properties of Cr(III) complexes with dipicolinic acid and 1,10-phenantroline, Polyhedron, 2008, 27: 502-512

Hamada, Y.Z., Carlson, B.L., Shank, J.T., 2003. Potentiometric and UV–Vis spectroscopy studies of citrate with the hexaquo Fe^{3+} and Cr^{3+} metal ions. Synth. React. Inorg. Met. Org. Chem. 33, 1425–1440.

Z. He, M.L. Zhu, G. Ma, 1,1-Dimethylbiguanidium tetrabromothallate(III), Acta Cryst. E, 2002, 58: m647-649.

Headlam, H.A., Lay, P.A., 2016. Spectroscopic characterization of genotoxic chromium(V) peptide complexes: Oxidation of Chromium(III) triglycine, tetraglycine and pentaglycine complexes. J. Inorg. Biochem. 162, 227–237.

Huang, Y., Rong, C., Zhang, R., Liu, S., 2017. Evaluating frontier orbital energy and HOMO/LUMO gap with descriptors from density functional reactivity theory. J. Mol. Model. 23 (1). https://doi.org/10.1007/s00894-016-3175-x.

Jain, S.K., Patel, P., Rogier, K., Jain, S.K., 2006. Trivalent Chromium Inhibits Protein Glycosylation and Lipid Peroxidation in High Glucose-Treated Erythrocytes. Antioxid. Redox Signal. 8 (1-2), 238–241.

Kim, D.-S., Kim, T.-W., Kang, J.-S., 2004. Chromium picolinate supplementation improves insulin sensitivity in Goto-Kakizaki diabetic rats. J. Trace Elem. Med Biol. 17 (4), 243–247.

Kuskov, A.N., Kulikov, P.P., Shtilman, M.I., Rakitskii, V.N., Tsatsakis, A.M., 2016. Amphiphilic poly-N-vynilpyrrolidone nanoparticles: Cytotoxicity and acute toxicity study. Food Chem. Toxicol. 96, 273–279.

P. Lemoine, A. Tomas, B. Viossat, D. Nguyen-Huy, Tétrachlorocuprate(II) de metformine, Acta Cryst. Sect. C, 1994, 50: 1437-1439.

P. Lemoine, M. Chiadmi, V. Bissery, A. Tomas, B. Viossat, Les Composés de la metformine avec les Ions CoII, CuII et NiII, Acta Cryst. Sect. C, 1996, 52: 1430-1436.

A. Levina, P.A. Lay, Chemical properties and toxicity of chromium (III) nutritional supplements, Chem. Res. Toxicol., 2008, 21: 563–571.

Levina, A., Lay, P.A., 2005. Mechanistic studies of relevance to the biological activities of chromium. Coord. Chem. Rev. 249 (3-4), 281–298.

Levina, A., Pham, T.H.N., Lay, P.A., 2016. Binding of Chromium(III) to Transferrin Could Be Involved in Detoxification of Dietary Chromium(III) Rather than Transport of an Essential Trace Element. Angew. Chem. Int. Ed. 55 (28), 8104–8107.

Z. Li, C.X. Liu, X. Xu, Q.Q. Qiu, X. Su, Y.X. Dai, J.Y. Yang, H.L. Li, W. Shi, C. Liao, M.B. Pan, W.L. Huang, H. Qian, Discovery of phenylsulfonyl acetic acid derivatives with improved efficacy and safety as potent free fatty acid receptor 1 agonists for the treatment of type 2 diabetes, Eur. J. Med. Chem., 2017, 138: 458-479.

Li, F., Wu, X., Zou, Y., Zhao, T., Zhang, M., Feng, W., Yang, L., 2012. Comparing anti-hyperglycemic activity and acute oral toxicity of three different trivalent chromium complexes in mice. Food Chem. Toxicol. 50 (5), 1623–1631.

Liu, W., Al-Oweini, R., Meadows, K., Bassil, B.S., Lin, Z., Christian, J.H., Dalal, N.S., Bossoh, A.M., Mbomekallé, I.M., de Oliveira, P., Iqbal, J., Kortz, U., 2016. Cr III -Substituted Heteropoly-16-Tungstates [Cr III2 (B -β-X IV W 8 O 31) 2] 14– (X = Si, Ge): Magnetic, Biological, and Electrochemical Studies. Inorg. Chem. 55 (21), 10936–10946.

Liu, L., Cui, W.M., Zhang, S.W., Kong, F.H., Pedersen, M.A., Wen, Y., Lv, J.P., 2015. Effect of glucose tolerance factor (GTF) from high chromium yeast on glucose metabolism in insulin-resistant 3T3-L1 adipocytes. RSC Adv. 5 (5), 3482–3490.

Liu, B., Liu, Y., Chai, J., Hu, X., Wu, D., Yang, B., 2016. Chemical properties and biotoxicity of several chromium picolinate derivatives. J. Inorg. Biochem. 164, 110–118.

Mahmoud, M.A., Zaitone, S.A., Ammar, A.M., Sallam, S.A., 2016. Synthesis, structure and antidiabetic activity of chromium(III) complexes of metformin Schiff-bases. J. Mol. Struct. 1108, 60–70.

S.M. El-Megharbel, Synthesis, Characterization and antidiabetic activity of chromium (III) metformin complex, J. Microb. Biochem. Technol., 2015, 7: 65-75.

Moghimi, A., Khavassi, H.R., Dashtestani, F., Kordestani, D., Ekram Jafari, A., Maddah, B., Moosavi, S.M., 2011. A ternary tetracoordinated Pd^{II} complex with metformin and dipicolinate: Synthesis, characterization and crystal structure. J. Mol. Struct. 996 (1-3), 38–41.

Mosmann, T., 1983. Rapid colorimetric assay for cellular growth and survival: Application to proliferation and cytotoxicity assays. J. Immunol. Methods 65 (1-2), 55–63.

K. Nakamoto, Infrared and Raman spectra of inorganic and coordination compounds, fifth ed. Wiley Interscience, New York, 1997.

Olar, R., Badea, M., Marinescu, D., Chifiriuc, M.-C., Bleotu, C., Grecu, M.N., Iorgulescu, E.-E., Lazar, V., 2010. N,N-dimethylbiguanide complexes displaying low cytotoxicity as potential large spectrum antimicrobial agents. Eur. J. Med. Chem. 45 (7), 3027–3034.

R. Olar, M. Badea, E. Cristurean, C. Parnau and D. Marinescu, Thermal behaviour of new N,N-dimethylbiguanide complexes having selective and effective antibacterial activity, J. Therm. Anal. Calorim., 2006, 84: 53-58.

Öztirk, Ö.F., Şekerci, M., Özdemir, E., 2006. Preparation of complexes of 1-amino-6,7-O-cyclohexylidene-4-azaheptane with transition metal acetates. Russ. J. Gen. Chem. 76 (1), 33–36. https://doi.org/10.1134/S1070363206010075.

Peng, M., Yang, X., 2015. Controlling diabetes by chromium complexes: The role of the ligands. J. Inorg. Biochem. 146, 97–103.

Preuss, H.G., Echard, B., Perricone, N.V., Bagchi, D., Yasmin, T., Stohs, S.J., 2008. Comparing metabolic effects of six different commercial trivalent chromium compounds. J. Inorg. Biochem. 102 (11), 1986–1990.

Rastegarnia, S., Pordel, M., Allameh, S., 2020. Synthesis, characterization, quantum-chemical investigation and antibacterial studies of new fluorescent Cr(III) complexes. Arabian J. Chem. 13, 3903–3909.

Ray, P., 1961. Complex Compounds of Biguanides and Guanylureas with Metallic Elements. Chem. Rev. 61 (4), 313–359.

Robles, E.F., Vázquez, V.P., Emiliano, J.R., Amaro, R.G., Briones, S. L., 2017. High fat diet induces alterations to intraepithelial lymphocyte and cytokine mRNA in the small intestine of C57BL/6 mice. RSC Adv. 7 (9), 5322–5330.

Schwarz, K., Mertz, W., 1957. A glucose tolerance factor and its differentiation from factor. Arch. Biochem. Biophys. 72, 515–518.

Schwarz, K., Mertz, W., 1959. Chromium(III) and the glucose tolerance factor. Arch. Biochem. Biophys. 85 (1), 292–295.

Sheldrick, G.M., 1996. SADABS an empirical absorption correction program. Bruker analytical X-ray systems, Madison, WI.

Sheldrick, G.M., 2008. A short history of SHELX. Acta Crystallogr A Found Crystallogr 64 (1), 112–122.

Stout, M.D., Nyska, A., Collins, B.J., Witt, K.L., Kissling, G.E., Malarkey, D.E., Hooth, M.J., 2009. Chronic toxicity and carcinogenicity studies of chromium picolinate monohydrate administered in feed to F344/N rats and B6C3F1 mice for 2 years. Food Chem. Toxicol. 47 (4), 729–733.

Sun, Y., Mallya, K., Ramirez, J., Vincent, J.B., 1999. The biomimetic $[Cr_3O(O_2CCH_2CH_3)_6(H_2O)_3]^+$ decreases plasma cholesterol and triglycerides in rats: towards chromium-containing therapeutics. J. Biol. Inorg. Chem. 4 (6), 838–845. https://doi.org/10.1007/s007750050357.

Tang, H.-Y., Xiao, Q.-G., Xu, H.-B., Zhang, Y.i., 2015. Hypoglycemic activity and acute oral toxicity of chromium methionine complexes in mice. J. Trace Elem. Med Biol. 29, 136–144.

Vincent, J.B., 2013. Chromium: is it essential, pharmacologically relevant, or toxic?. Met. Ions Life Sci. 13, 171–198.

Vincent, J.B., 2015. Is the Pharmacological Mode of Action of Chromium(III) as a Second Messenger?. Biol. Trace Elem. Res. 166 (1), 7–12. https://doi.org/10.1007/s12011-015-0231-9.

C. Wang, Z.Q. Chen, Y.X. Pan, X.D. Gao, H.X. Chen, Anti-diabetic effects of inonotus obliquus polysaccharides-chromium(III) complex in type 2 diabetic mice and its sub-acute toxicity evaluation in normal mice, Food Chem. Toxicol., 2017, 108: 498-509

Wang, Y.-Q., Yao, M.-H., 2009. Effects of chromium picolinate on glucose uptake in insulin-resistant 3T3-L1 adipocytes involve activation of p38 MAPK. The Journal of Nutritional Biochemistry 20 (12), 982–991.

Weeks, C.L., Levina, A., Dillon, C.T., Turner, P., Fenton, R.R., Lay, P.A., 2004. Synthesis and Characterization of a Chromium(V) cis -Dioxo Bis(1,10-phenanthroline) Complex and Crystal and Molecular Structures of Its Chromium(III) Precursor. Inorg. Chem. 43 (24), 7844–7856.

L.E. Wu, A. Levina, H.H. Harris, Z. Cai, B. Lai, S. Vogt, D.E. James, P.A. Lay, Carcinogenic chromium(VI) compounds formed by intracellular oxidation of chromium(III) dietary supplements by adipocytes, Angew. Chem. Int. Ed., 2016, 55: 1742-1745.

Zhu, M., Lu, L., Jin, X., Yang, P., 2002. Trichloro(1,1-dimethylbiguanidium-κ N^3)zinc(II). Acta Crystallogr C Cryst Struct Commun 58 (3), m158–m159.